ESCUELA DE CONSTRUCCIÓN CIVIL
FACULTAD DE INGENIERÍA
Revista de la Construcción
Journal of Construction

Research Article

Investigation of plastic hinge length in high-ductility reinforced concrete shear walls

Hacer Tülen [1]*, Yunus Dere [2], Musa Hakan Arslan [3]

[1] Department of Civil Engineering, Kocaeli University, Kocaeli (Turkey), email: hacer.tulen@kocaeli.eu.tr
[2] Department of Civil Engineering, Necmettin Erbakan University, Konya (Turkey), email: ydere@erbakan.edu.tr
[3] Department of Civil Engineering, Konya Technical University, Konya (Turkey), email: mharslan@ktun.edu.tr
*Correspondence: hacer.tulen@kocaeli.edu.tr (T. Hacer)

Received: 28.12.22; **Accepted:** 05.12.24; **Published:** 31.08.24

Citation: Tülen, H., Dere Y., Arslan, M.H. (2024). Investigation of plastic hinge length in high-ductility reinforced concrete shear walls. Journal of Construction, 23(2), 177-202. https://doi.org/10.7764/RDLC.23.2.177

Abstract: In this study, the plastic hinge lengths of reinforced concrete (R/C) cantilever shear walls were analytically determined considering various design parameters. Nonlinear static (Pushover) analyses were conducted on R/C shear wall models and their nonlinear behavior was examined using ABAQUS software. In the study, 72 shear wall models with different parameters were analyzed under the influence of vertical and horizontal loads. Parameters whose effects on plastic hinge length were investigated height/length ratio (H_w/L_w), axial load ratio (N/N_o), and horizontal web reinforcement ratio (ρ_{sh}). The load-displacement graphs of the modelled shear walls were obtained. The plastic hinge height of shear walls was determined according to the heights of the deformations in the concrete and longitudinal steel reinforcement in the section when the shear walls lateral load decreased by 15%. The analytical plastic hinge lengths (L_{pz}) were determined with respect to the location of the yield occurred at the longitudinal steel reinforcement of the shear wall. The observed plastic hinge lengths (L_p) were determined based on the height of observed the crush as of the foundation top level in the concrete shear wall model. The relationship between the findings of this study and empirical formulas in the literature was determined. It was determined that there is greater closeness between the values obtained from empirical formulas in the literature and the observed plastic hinge length values. It was observed that the plastic hinge length generally increases as the shear span increases. It was observed that the change in ρ_{sh} was not a very effective parameter in plastic hinge formation. As the N/N_o decreases, the plastic hinge length values generally increase. The L_p/L_{pz} ratio varied within the range of 0.15-0.50. In addition to ductility (μ) values were determined by using the displacements determined according to both the crushing occurred in the shear wall concrete and the yield observed in the steel reinforcement. The observed that the ductility value depends more on H_w/L_w ratio as N/N_o ratio decreases.

Keywords: Earthquake, failure, plastic hinge, finite elements, shear wall.

1. Introduction

Mechanical models that can predict the analytical load-deformation relationship with sufficient accuracy must be used for the evaluation of the behavior of the reinforced concrete structures under earthquake. In order to obtain the more realistic load-displacement relationship of structures, the behavior of non-linear regions must be modeled within the framework of a set of rules. In the computer models of structures, plastic hinge assumptions are made for the regions where plastic deformations are anticipated to occur. In a plastic hinge of reinforced concrete section, the reinforcement in the tension zone must first yield and then the concrete in the compression zone must be crushed with the increasing curvature demand. The region

where the plastic hinge forms and the height (length) of the plastic hinge are extremely important to determine the global performance of a structure. Aksoylu et al. (2020) conducted pushover analyses for structures with different story heights and investigated the formation of plastic hinges Eslami & Ronagh (2014), Değer & Başdoğan (2020) stated that the features adopted for the plastic hinge change the load-displacement relationship of a structure. In order to obtain the accurate load-displacement relationship of a building, the hinge-development features of shear walls, columns and beams, which form the load carrying system, are important. Moreover, it is also known that especially shear walls play an important role in the horizontal load bearing capacity and the ductility of a building during earthquake.

Reinforced concrete shear walls are frequently preferred in countries with high seismic activity in order to increase the horizontal stiffness of the structural system and to reduce the displacements taking place during the earthquake and the damages associated with them (Sorosh & Sari (2022)). In order to ensure the performance expected from shear walls during earthquake is achieved, it is extremely important to design the shear walls with adequate reinforcement and place them at appropriate locations within the building. Field observations after earthquakes, such as 06 Şubat 2023 Kahramanmaraş Earthquake Doublets (7.8 M_w and 7.6 M_w in Turkey) have documented that malpractice actions in especially improperly selection of shear wall locations, inadequate reinforcement detailing and weak workmanship for concrete triggered to damage (Marius, 2013; İTÜ, 2023; Oztürk et al., 2023). Similarly, Kam et al. (2011) and Ozdemir et al. (2021) point out, especially based on their field observations made after earthquakes, that there were not enough shear walls in the buildings where high damage and destruction occurred. In the Turkish Building Earthquake 2018 (TBEC-2018) and other previous versions, no shear wall area condition is given depending on the building height and ground floor area (except for tunnel formwork buildings). Additionally, there are empirical approaches considering wall density in the literature (Kazaz, 2016; Soydaş, 2009; Alkazan, 2020; Burak & Comlekoglu, 2013) recommendations are given about the amount of shear walls to prevent the collapse of a reinforced concrete building.

There are different studies in the literature on the seismic behavior of shear walls. Gallegos et al. (2023) evaluated the seismic collapse behavior of high-rise RC dual-wall-frame buildings located on moderately stiff soil. Sritharan et al. (2014) investigated the weaknesses and design principles of shear walls in earthquake behavior. Henry (2013), Lu et al. (2017), Encina et al. (2016), Lu et al. (2018) examined the effect of longitudinal reinforcement placement in shear walls on behavior. Dazio et al. (2009) investigated different vertical reinforcement and ductility content in shear wall. Kazaz (2013), Takahashi et al. (2013), Massone & Alfaro (2016), Foroughi & Yüksel (2020) investigated the effects of changing parameters on the nonlinear behavior of shear walls. Cai et al. (2024) investigated the plastic hinge lengths of flanged reinforced concrete walls using the finite element method. They proposed equations for determining the plastic hinge length by taking into account the effects of different parameters. Jun (2014) investigated the damage conditions of the shear wall with the fiber element method. The general purpose of these studies is to determine the parameters that affect the seismic behavior of shear walls. In addition, determination of plastic hinge height has been the main motivation subject.

In order to dissipate energy, the structure needs to undergo plastic deformations during an earthquake. In regions where plastic deformations occur, crushing in concrete deformations in compression zone can be observed from the outside of shear walls, whereas it is not possible to observe starting point of steel longitudinal bars yield deformations. In other words, in the section, the plastification starts from the point where the reinforcement yields and it is impossible to observe this length from the outside. If concrete and reinforcement damage are evaluated separately, plastic hinge height can be considered in two ways as the height at which the concrete is crushed (observed height, L_p) and the height at which the reinforcement longitudinal bars start to yield (analytical height, L_{pz}). However, the number of studies investigating the relationship between L_p and L_{pz} depending on the parameters is very limited.

Observations made in the field after earthquakes and data obtained from experimental studies indicate differences between the plastic hinge length L_p obtained from external observation and the plastic hinge length L_{pz} formed starting from the section where longitudinal reinforcement is yielded (Priestley et al. 2007; Bohl and Adebar, 2011). Certainly, it is evident that in experimental studies, deformation measurement can be performed by placing strain gauges on longitudinal reinforcements close to the outermost fiber in the tension zone (Dazio et al., 2009). However, experimental data on this is quite limited. Especially in experiments, the negative effect of strain-guage placement on bond challenges researchers on this issue

(Hoffmann, 2012; Clauß et al., 2020). In this respect, by calculating the distance to the foundation of the sections where the reinforcement yielded and the concrete begins to crush, with developed FEM methods, the lengths of both plastic hinges (L_p and L_{pz}) can be calculated without performing experiments.

There are many parameters depending on the properties of the shear wall that affect the difference between L_p obtained from observed and L_{pz} obtained analytically. The main purpose of this study is to see the interaction between L_p and L_{pz}. In other words, it is very important to calculate the relationship between the plastic hinge height L_p, formed by crushing the concrete, and the final section height L_{pz}, where the reinforcement yielded, through a non-linear FEM model developed. In the study, also aimed to compare the relationship between the L_p and L_{pz} values obtained from empirical formulas in the literature and the values founded in this study.

For this reason, in the study, it was aimed to analytically (by using FEM) determine the plastic hinge lengths of high-ductility shear walls. The numerical analysis provides a deeper understanding of the structural behavior and allows collecting data which is difficult to record during the experiments and it is utilized as an alternative to the experimental study by many researchers (Pokhrel and Bandelt (2019), Barbagallo (2022). It is preferred various software to examine building behavior in the literature. Zhao et al. (2011) used the DIANA program to examine the plastic hinges formed in beams in terms of element dimensions, reinforcement ratio and material properties. Zhang et al. (2022) examined the behavior of prestressed concrete composite shear walls according to various parameters with Abaqus software. Mamdouh et al. (2022) used the ANSYS finite element program to examine the behavior of reinforced concrete shear walls with discontinuities. In this present study, numerical analyses were performed using a finite element tool, ABAQUS, to deeply investigate the effects of the parameters on L_p and L_{pz} of ductile reinforced concrete shear walls. In this study, concrete and material models were selected by the authors from models previously used in the verification of various experimental studies. L_p and L_{pz} interpretations were made based on the damage distribution and deformation profile obtained as a result of the analysis of 72 different shear walls. Moreover the shear walls were modeled by ABAQUS software and the load-displacement graphs of each shear wall were obtained. Despite there are many studies in the literature about shear wall L_p and L_{pz} lengths, the associations made based on concrete and reinforcement deformation through the FEM-model used and the commentations made about μ_δ have not been discussed in the literature. Therefore, the novel part of the study is to obtain the L_p and L_{pz} relationship depending on concrete and reinforcement deformation, and to examine the L_p and L_{pz} relationship according to the changing parameters in this context.From this motivation, first of all based on a shear wall sample tested in the literature, the numerical model verified. After that seventy-two (72) shear walls were designed and modeled according the requirements stipulated in the TBEC-2018 and selected parameters. While determining the parameters whose effects will be examined, the literature was examined. The studies have shown that there are different expressions for the plastic hinge length for each distinct parameter such as wall length (L_w), wall height (H_w), axial load level (N/N_o), and the ratio of moment to shear force. There are different opinions about change of L_p when the height/length ratio (H_w/L_w) ratio of the shear walls becomes greater than 2. However, there is no direct expression that takes into account the effect of the change of the H_w/L_w ratio on the plastic hinge length. For this reason, the H_w/L_w ratio was determined as a parameter in the study. Other parameters taken into account were axial load ratio (N/N_o) and horizontal web reinforcement ratio (ρ_{sh}). The codes provide limit values for these parameters, and their effects have been studied as they are crucial for determining the plastic hinge length in accordance with the actual behavior. In the study, nonlinear analyses were conducted on 72 different types of shear wall sections when the tested parameters were selected as L_w, H_w, N/N_o, and ρ_{sh}. Certainly, other factors may be effective in determining the behavior of shear walls. For example, wall thickness, slab type, slab-shear wall connection type are some of them. The plastic hinge height of shear walls was determined according to the heights of the deformations in the concrete and longitudinal steel reinforcement in the section when the shear walls lateral load decreased by 15%. The relationship between the findings of this study and empirical formulas in the literature was determined. Displacement ductility (μ_δ) of shear walls were also determined with respect to selected parameters.

2. Description of plastic hinge

During an earthquake, reinforced concrete structures undergo non-linear deformations. It is assumed that nonlinear flexural deformations in buildings concentrate at the sections called plastic hinge (the assumption of lumped plastic damage), and the system behaves elastically in the remaining regions. This hypothesis is called the plastic hinge hypothesis (Kumbasaroğlu, 2010).The plastic hinge length of a shear wall modeled as a vertical cantilever as shown in Figure 1 can be calculated as the sum of the elastic displacement at yielding state at the top of the shear wall (Δ_y) and the plastic displacement arising from the rotation of the plastic hinge (Δ_p). The method of calculation of the rotation value is presented in Equation 1.

$$\Delta = \Delta_y + \Delta_p = \frac{\emptyset_y H_w^{\,2}}{3} + (\emptyset_u - \emptyset_y)\, L_p(\, H_w\text{-}0.5L_p) \tag{1}$$

In the above equation, $\emptyset_y$ represents the yield curvature and $\emptyset_u$ represents the final curvature, and the L_p component allows to determine the plastic hinge rotation angle. It is assumed that the plastic curvature is lumped in the middle of the L_p. For this reason, the total length was taken as (H_w-0.5L_p) in the plastic displacement calculation. L_p, which is also defined as the observation length where sectional damages gather (where theoretical crush occurs in the concrete) after earthquakes, in fact does not exactly represent the point where plastification occurs. Within the section, the plastification starts from the point where the reinforcement yields. The height (L_{pz}) of this area, where reinforcement begins to yield, can become higher than the length of the plastic hinge (Kazaz, 2013; Kazaz & Gülkan, 2012). However, it is impossible to observe this length from the outside. For this reason, strain gauges must be placed on the reinforcement. Priestley et al. (2007), Hoult el al. (2018) and Kazaz (2013) accepted the L_{pz} length as 2L_p in their studies (Kazaz & Gülkan, 2012). Similarly, in this study, L_p was defined as the observed plastic hinge height and the L_{pz} was defined as the calculated (analytical) plastic hinge height. The main purpose of the study is to formulate the relationship between L_{pz} and L_p depending on changing shear wall parameters.

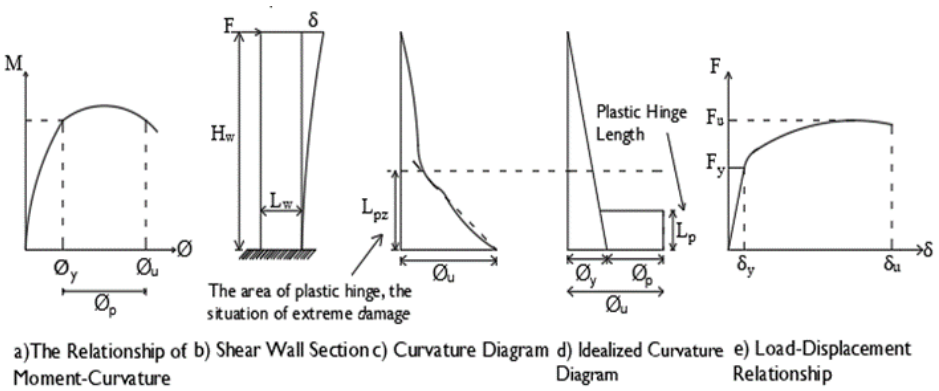

Figure 1. Plastic hinge method and definition of hinge length (authors).

Shear wall height is an important parameter in the plastification of shear walls. When the H_w/L_w ratio is greater than 2, bending behavior is generally observed for the shear wall. TBEC-2018 (2018) and other codes (ACI-318 (2019) ; Eurocode-8 (2004)) accepted the situation of (H_w/L_w) ratio being equal to 2.0 as the limit state. In the literature there are different opinions about L_p when the H_w/L_w ratio of the shear walls becomes greater than 2. Kazaz & Gülkan (2012) developed Equation (2) to determine the plastic hinge length, taking into account other variables as well.

$$L_p = 0.27\, L_w \left(1-\frac{N}{N_0}\right)\left(1-\frac{f_y}{f_c}\rho_{sh}\right)\left(\frac{\frac{M}{V}}{L_w}\right)^{0.45} \tag{2}$$

In Equation (2), N/N_o is the axial load ratio at the base of shear wall, ρ_{sh} is horizontal web reinforcement ratio, M/V is moment to shear force ratio, L_w is shear wall length, f_c is concrete compressive strength, f_y is reinforcement yield strength, and (M/V) /L_w ratio takes into account shear wall's failure mode (bending, shearing, shearing / bending) and to some extent replaces the shearing stress. Biskinis & Fardis (2010) proposed Equation (3) for the members that have good seismic detailing.

$$L_p = 0.2L_w\left(1 + \frac{1}{3}\min\left(9, \frac{L_s}{L_w}\right)\right) \quad (3)$$

where, L_s/L_w ratio is the ratio of moment shearing force to shear wall width. Bohl and Adebar (2011) proposed Equation (4).

$$L_p = (0.2L_w + 0.05L_s)\left(1 - 1.5\frac{N}{A_g f_c}\right) \leq 0{,}8L_w \quad (4)$$

where, N is axial load, A_g is shear wall area in earthquake direction. Eurocode8 (2004) proposes the plastic hinge length be determined by Equation (5).

$$L_p = \frac{L_s}{30} + 0.2L_w + 0.11\frac{d_{bL} f_y(MPa)}{\sqrt{f_c\,(Mpa)}} \quad (5)$$

where, L_s is the shearing span (M/V), d_{bL} is average reinforcement diameter. Altheeb et al. (2015) used Equation (6) to determine the plastic hinge length. In the equation f_u is reinforcement ultimate strength and f_c' compressive strength of concrete.

$$L_p = \frac{(f_u - f_y)d_{bl}^2}{4\sqrt{f_c'}} \quad (6)$$

Aydın (2018) examined the plastic hinge lengths and displacement limits by considering the moment curvature relations of the shear walls. Zhi et al. (2019) examined behavior of reinforced concrete shear walls with continuous or lap-spliced bar connections in plastic hinge zones. Foroughi & Yüksel (2019) investigated the effects of different parameters on plastic hinge length and displacements through analytical models. Hashim et al. (2020) investigated the plastic hinge lengths of curtains by creating finite element models.

2.1. *Relationship between critical shear wall height and plastic hinge length*

If a reinforced concrete building contains shear walls, shear wall damage is primarily expected in an earthquake. Example shear walls that are damaged during earthquakes are shown in Figure 2. Figure 2b.(a) shows a shear wall damaged in 2011-Canterbury earthquake, Figure 2(b) shows a shear wall severely damaged in 2010-Maule earthquake and Figure 2(c) shows another shear wall severely damaged in 2010-Chile earthquake. Damages in Figure 2b.(b) and Figure 2b.(c) were caused by incorrect detailing of the shear walls (These shear walls have not been designed according to the relevant regulations). The aim of this study is to determine the L_p and L_{pz} lengths of the shear wall designed according to the codes. After the shear walls are damaged, the displacements will increase in the structures and frame elements starts to experience damage. If there is no strength to meet the displacement made by the shear wall at the column flange regions, there may be hinge development at column flanges and the situation may cause the structure to collapse. In order to prevent such a situation, the amount of bending displacements expected to occur in the plastic hinge zones, and the distribution of the damage must be taken into consideration during the design of ductile shear walls.

(a) (b) (c)

Figure 2a. Examples of reinforced concrete shear walls damaged after 2023 Kahramanmaraş Earthquake Doublet; (Oztürk et al. (2023).

(a) (b) (c)

Figure 2b. Examples of reinforced concrete shear walls damaged in earthquakes (Grossi et al., 2011); (Westenenk, B. et al., 2012).

In order to prevent the brittle collapse mechanism and limited ductility, the plastic hinge zones that may be formed should be properly detailed. In order for this detailing to be proper, the codes introduced some limits in the areas where they expect shear wall stresses to be maximum and defined the critical shear wall height. Table 1 shows the formulas for critical shear wall height in TBEC-2018 (2018) and ACI 31 (2019) and EC8 (2004) codes. The reinforcement distribution is denser along the critical height and it was required to create shear wall flange regions when the H_w / L_w ratio is greater than 2. In other words, if the ratio remains below 2, flexural hinging development is not expected in the shear wall.

Table 1. Critical shear wall height limits determined by codes.

References	Critical shear wall height (H_{cr}) limits
TBEC-2018	$2L_w \geq H_{cr} \geq \max(l_w; H_w/6)$
EC8-2005	$H_{cr} = \max(L_w; Hw/6), 2L_w$ $H_{cr} \leq h_s$ n≤ 6 stories $2h_s$ n≥7 stories
ACI- 318-2019	$H_{cr} = (L_w; M_u / 4V_u)$

(L_w: Length of shear wall in the plan, H_w: Total shear wall height, h_s: story height, n: number of stories, M_u: Moment value in shear wall section, V_u: Shearing force in shear wall section)

2.2. *Ductility and plastic hinge length*

Ductility is the ability of a material, section, element, or a structural system to strain beyond the elastic limit, thus, to displace, without any significant change in stress, section force, or load. Plastic hinge length and, member and system ductility are closely associated with. The requirement of ductility is the formation of plasticization zones. Inel and Ozmen (2006) and, Arslan (2012) observed, in their studies, that the plastic hinge length affects the displacement capacity, consequently affectings

the ductility. In Figure 3, F_u stands for the ultimate load, δ_y for yield displacement where elastic behavior ends, δ_u for ultimate displacement, and the numerical definition of ductility is expressed by Equation (7).

The accuracy of the models created for structures can be determined by load-displacement curves. Load displacement curves provide information about the behavior of structural elements. Figure 3 shows the information that can be determined with the help of the load-displacement curve along with ductility. The plastic hinge height of shear walls was determined according to the heights of the deformations in the concrete and longitudinal steel reinforcement in the section when the shear walls lateral load decreased by 15%. Displacement ductility (μ_δ) of shear walls were also determined with respect to selected parameters.

For ductility comparison, the maximum displacements that the shear wall can achieve without any major loss in capacity are taken into account. Therefore, the ductility ratio is calculated as the ratio of the displacement value (δ_u) corresponding to 85% of the maximum load-carrying capacity attained by the beam to the displacement value at yielding (δ_y) for flexural RC elements. It is stated in the literature that the minimum value of this ratio for a RC member is around 4 ~ 5 (Ling et al. (2023)). Shear walls where shear behavior is effective on the other hand, ductility is quite limited since no ductile plateau will occur.

$$\mu_\delta = \frac{\delta_u}{\delta_y} \qquad (7)$$

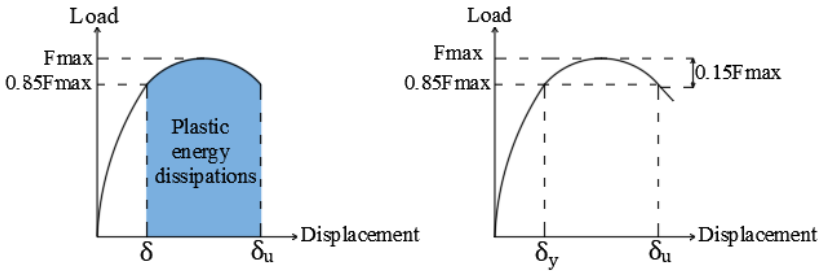

Figure 3. Energy dissipation capacity and load-displacement relationship.

3. Analytical study

In this present study, numerical analyses were performed using a finite element tool of ABAQUS to i) investigate the effects of the parameters on L_p and L_{pz} of ductile reinforced concrete shear walls, ii) determine the plastic hinge lenghts of high-ductility shear walls, iii) evaluate the damages (crushing of concrete and yielding of steel) separately for concrete and reinforcement and to determine the relationship between L_p and L_{pz}, iv) determine displacement ductility of shear walls with respect to selected parameters. The parameters selected in the study to achieve these four objectives are explained below. The selected parameters are similar to the parameters studied in the literature. Slab thickness, concrete class, longitudinal reinforcement ratio, shear wall thickness, conditions in the connection area, etc. many parameters such as can also affect the results These parameters were kept constant due to the limits of the study.

In the experimental and analytical studies in the literature by Thomsen & Wallace (2004), Biskinis & Fardis (2010), Bohl & Adebar (2011), Kazaz & Gülkan (2012), the amount of the effect of these parameters was discussed and they proposed empirical formulas. The parameters included in the formulas are shown in Table 2. The parameters considered in this study and their ranges of variation are shown in Table 3. 72 shear wall models were examined in the current study.

Table 2. Parameters in formulas suggested in the literature (authors).

Literature	Parameters				
	L_w	H_w	M/V	N/N_o	ρ_{sh}
Thomsen and Wallace (2004)	✓				
Biskinis & Fardis (2010)	✓		✓		
Bohl ve Adebar (2011)	✓		✓	✓	
Kazaz & Gülkan (2012)	✓		✓	✓	✓

Table 3. Selected parameters and their ranges (authors).

Parameter	Min	Max	Step of increase
H_w/L_w	2	7	1
ρ_{sh}	0.0015	0.0035	0.0010
N/N_o	0.05	0.20	0.05

3.1. Design of the reinforced concrete shear walls

Calculations were made by taking the thickness of the shear walls (b_w) as 0.25 m and the length of the shear walls in the plan (L_w) as 1.75 m, by taking into consideration the cross-section limiting conditions given in TBEC-2018.

The shear wall models were created with the critical shear wall height (H_{cr}) being 1.76 m for all shear walls whose H_w/L_w ratio is different from 2. In shear walls whose H_w/L_w ratio is greater than 2, flange regions were created. The length of the shear wall flanges was determined as 0.50 m along the critical shear wall height, and as 0.25 m above the critical shear wall height.

Steel reinforcement was determined using the minimum reinforcement ratios according to TBEC-2018. The design was made so that the longitudinal reinforcement is 16Ø10 in the shear walls with H_w/L_w=2. The reinforcement used in the shear walls whose H_w/L_w ratio is greater than 2 are given in Table 4. The details of a sample shear wall reinforcement whose H_w/L_w ratio is 4 is given in Figure 4.

Table 4. Reinforcement used in shear walls whose H_w / L_w ratio is greater than 2 (Authors).

Location	ρ_{lu}	ρ_{lw}	ρ_{sh}
$H<H_{cr}$	6Ø14	6Ø10	Ø10/42(0.0015) Ø10/25(0.0025) Ø10/18(0.0035)
$H>H_{cr}$	4Ø14	10Ø10	

(ρ_{lu}: flange longitudinal reinforcement at critical height, ρ_{lw}: flange reinforcement above critical height, ρ_{sh}: horizontal web reinforcement)

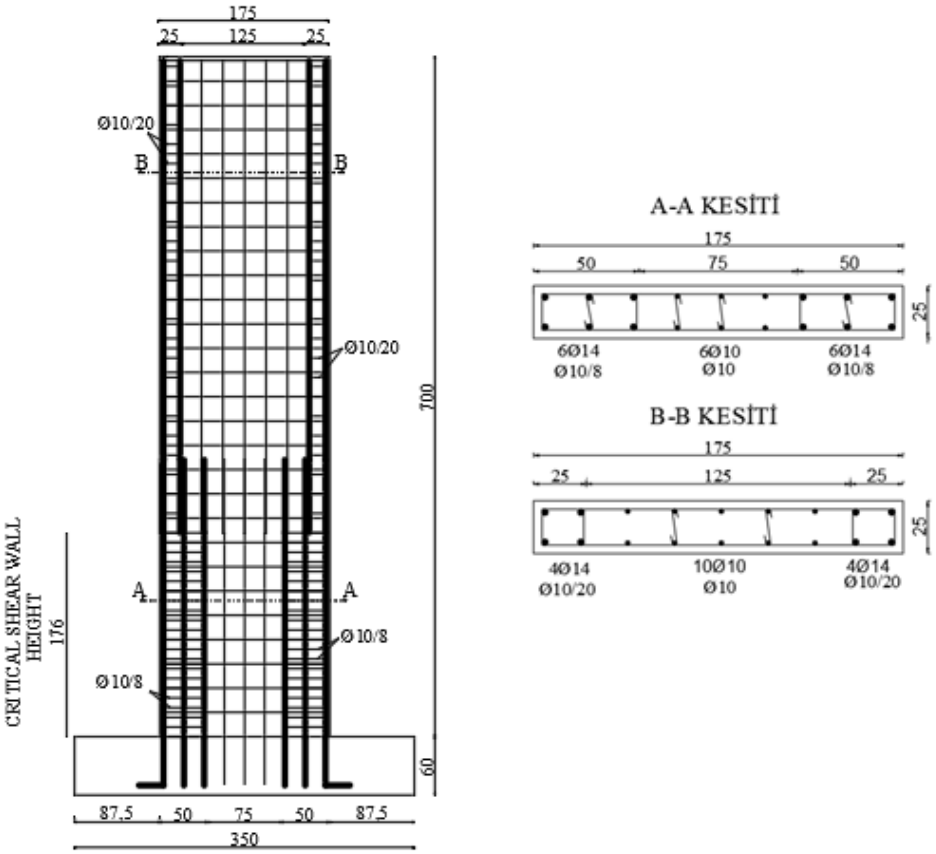

Figure 4. Shear wall reinforcement detail (authors).

3.2. Design of the reinforced concrete shear walls

Microscopic models are used to evaluate the behavior of the reinforced concrete shear walls. They take into account continuous mechanics and often include solutions with numerical processing procedures. Finite elements may be cited as examples for microscopic models (Marzok et al., 2020). Shear wall models were created within ABAQUS, which is commercial finite element software. The concrete part of the shear walls was modeled by using solid finite elements and their reinforcements were modeled with truss elements.

In the study, the concrete grade is chosen as C25 (compressive strength (f_{cd}) is 25 MPa, and reinforcement type B420c (yield strength is 420 MPa). The formulas given in Dere (2017) were used for the compressive and tensile behavior of concrete. In Figures 5-6, uniaxial stress-strain curves are given for concrete and steel. The damage parameter referred to in CDPM material definition expresses the damage ratio, occurring in the element, with real numbers between 0-1. The relationship between the inelastic strain and the damage parameter of tensile and compressive behavior of concrete, were calculated based on the formulas given in Dere (2017). Figure 7 shows the damage parameter variation graph obtained for the concrete compression behavior. The TS500-2000 (2000) and ACI-318 (2019) codes accept the strain corresponding to the uniaxial compressive strength of the concrete as 0.003 for all concrete grades. A confined concrete model has not been created since the lateral web reinforcements inside the shear wall and stirrups at the wall flange regions are modeled in ABAQUS. Therefore, the web concrete was modeled as unconfined. In other words, the reinforcement is already defined in the model, the behavior of confined and unconfined concrete emerges in the ABAQUS model.

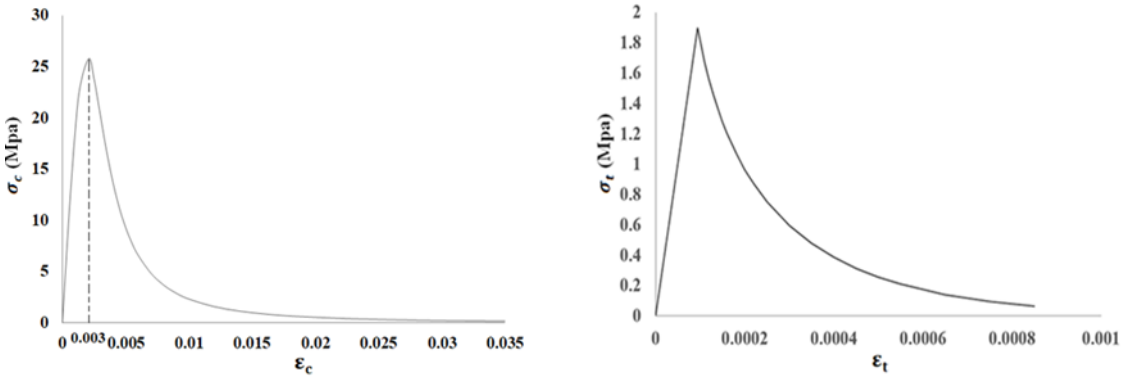

(a) (b)

Figure 5. Uniaxialstress-strain relationship of concrete ; (a) for compression, (b) for tension (authors).

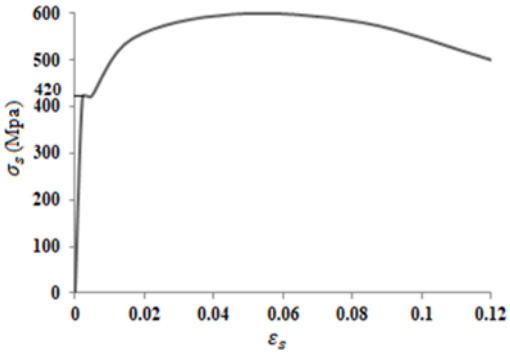

Figure 6. Uniaxial stress-strain relationship for steel (authors).

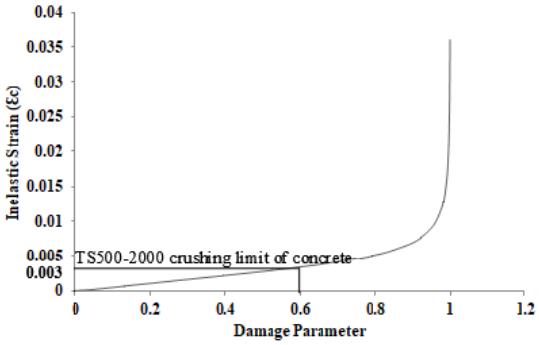

Figure 7. Compressive damage parameters (authors)

Load definitions were made so that N/N_o become 0.05, 0.1, 0.15, and 0.2. The supports were arranged as fixed supports. Top horizontal displacements of the shear walls considered in plastic hinge length calculation were determined according to the displacement corresponding to the collapse of the shear wall.

Damage modes of shear walls can be divided into two types: in-plane and out-of-plane damage. Due to the earthquake effect, most of the shear walls exhibited in-plane damage. However, there are shear walls that are damaged out of plane under certain earthquakes. For shear walls with small thicknesses, out-of-plane damage may occur even when the inter-story deformation in the out-of-plane direction is small (Cheng et al. (2023)). Robazza et al. (2018), El-Hashimy et al. (2020) and Wang et al. (2021), examined the out-of-plane behavior of shear walls. However, existing studies and finite element analyzes less consider the contribution of the out-of-plane stiffness of shear walls (Wei et al. (2017)). In this study, out-of-plane behavior is neglected.

A mesh sensitivity analysis was carried out in order to optimize maximum solid finite element size. The finite element mesh size was changed from 30 mm to 80 mm as presented in the table. In the example analysis, the top surface of the shear wall was subjected to a 20 mm lateral displacement, and a nonlinear pushover analysis was carried out. The results for all mesh configurations were presented in the Table 5. As it is seen, the base shear obtained from config #1 and config #3 are quite close. The concrete material used in the analyses is nonlinear and therefore the variation of the base shear is not as expected to be (as the number of nodes increases). The analysis of config #1 took around 11 hours whereas the analysis of config #3 took around 2 hours and 40 minutes. Therefore config #3 was found to be accurate enough and convenient in terms of computation time. Truss reinforcement elements were divided into 0.05 m wide finite elements (Figure 8).

Table 5. The effect of using various mesh size.

Mesh configuration No.	Maximum element size (mm)	Number of nodes	Number of elements	Top edge displacement (mm)	Base shear (kN)
1	30	221021	195952	19.5362	157.967
2	40	102941	88620	19.5347	159.610
3	50	59848	50641	19.5366	157.656
4	60	38376	32010	19.5349	159.796
5	70	30796	25919	19.5356	159.758
6	80	22723	19022	19.5349	160.310

In order to be able to perform the displacement-controlled analysis of the modeled shear walls the displacement loading was applied monotonically. The assumption of complete bond between concrete and reinforcement has been made. The displacement contour was used to determine the value of concrete damage occurring in the pressure zone. Coloring in the output was examined for damage parameters corresponding to inelastic strain of 0.003 and larger.

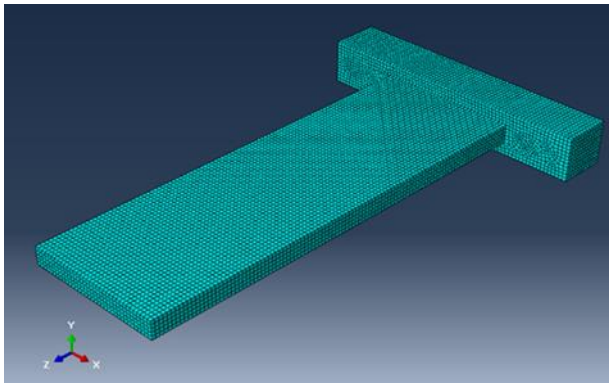

Figure 8. Dividing the shear wall model into finite elements (authors).

The accuracy of the used software and the created models were checked against the experimental results of the RW2 shear wall test with an H_w/L_w ratio of 3 conducted by Thomsen and Wallace (2004) (Figure 9 and Figure 10). An axial load of $0.07A_g f_c^{'}$ was applied at the top of the RW2 shear wall. In additon lateral displacements was applied to the top of the shear wall. As a result of the experiment, the damage situation occurred when the RW2 shear wall makes 2.5% drift is shown in Figure 10 (Thomsen & Wallace, 2004). As can be seen in the ABAQUS model, 15% strength loss after maximum lateral load corresponds to 2-2.5% lateral displacement ratio.

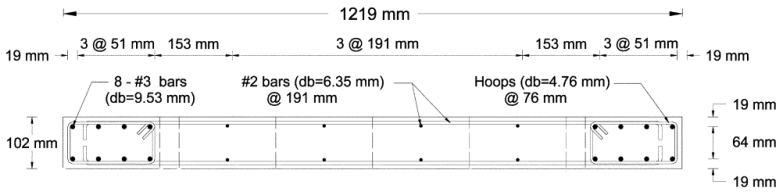

Figure 9. RW2 shear wall cross-sectional view (Thomsen & Wallace, 2004).

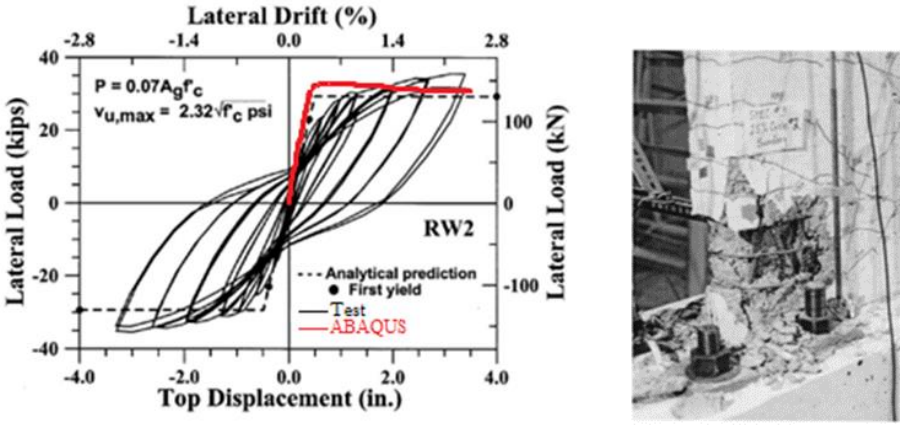

Figure 10. Comparison of load displacement curves-RW2 and RW-2 damage-2.5% drift. (Thomsen & Wallace, 2004).

Load-displacement curves of the modeled shear walls were obtained. In determining the plastic hinge lengths the horizontal displacement level at the moment when the maximum load decreases by 15% which is assumed to correspond to the collapse of the shear wall was used.

Considering the damages occurred in the reinforcement and concrete at the determined displacement values, the plastic hinge lengths for the shear walls were determined as two different height values, L_p and L_{pz} (Figure 11 and Figure 12).

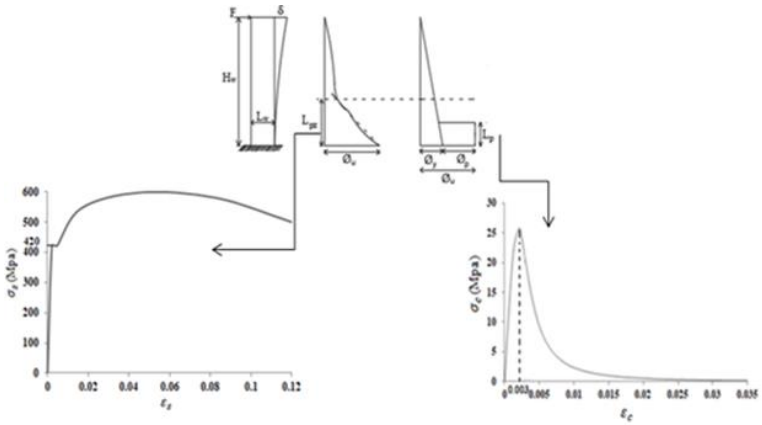

Figure 11. L_{pz} and L_p's theoretical illustration on the shear wall (authors).

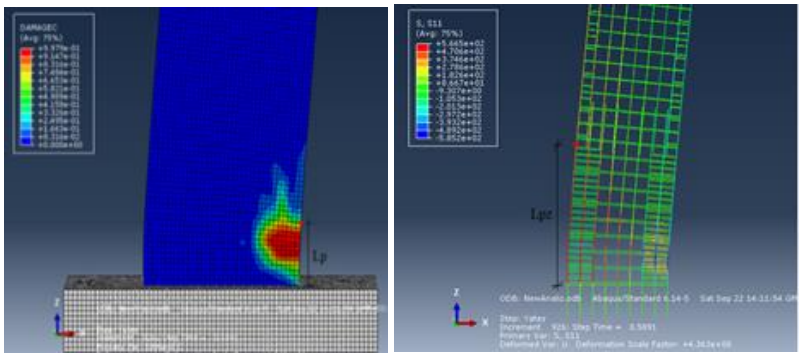

(a) (b)

Figure 12. Illustration of the plastic hinge lengths on the shear wall model; (a)L_p, (b)L_{pz} (H_w/L_w 7-ρ_{sh} 0.0035-N/N_o 0.15) (authors).

4. Research results

The plastic hinge lengths, evaluated for each shear wall at the determined displacement values, were calculated as L_p and L_{pz}. Examples of damage situations taken into account when determining L_p values are shown in Table 6 and Table 7. In the tables arranged according to the N/N_o ratio, it is seen that the concrete damages are concentrated in the pressure zone of the shear walls. However, at low load level (N/N_o=0.05), deformation also occurred in the concrete in the tension zone. Load level change causes changes in damage distribution. It is seen that as the N/N_o ratio increases, the damage occurs in a narrower area. L_p lengths were determined according to the damage status of the outermost fiber in the concrete. The effect of horizontal web reinforcement ratio could not be observed in the damage patterns, since the behavior of unconfinement concrete was observed in the outermost fiber of the concrete.

Table 6. Examples of damage cases when ρsh value is 0.0015 for L_p (authors).

H_w/L_w= 4, ρ_{sh} =0.0015			
N/N_o=0.05	N/N_o=0.1	N/N_o=0.15	N/N_o=0.2
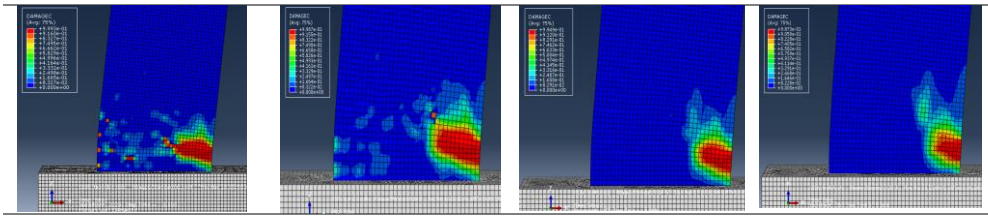			
H_w/L_w= 6, ρ_{sh} =0.0015			
N/N_o=0.05	N/N_o=0.1	N/N_o=0.15	N/N_o=0.2
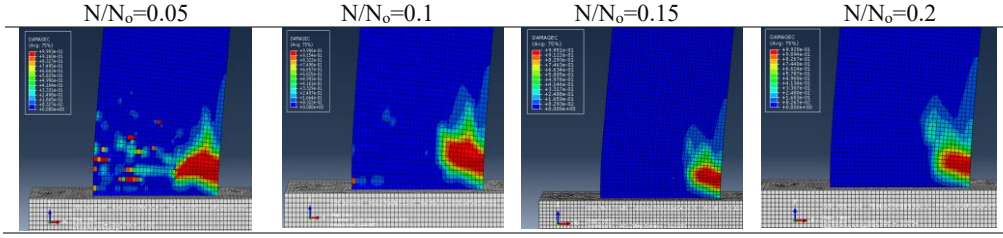			

Table 7. Examples of damage cases when ρsh value is 0.0035 for L_p (Authors)

H_w/L_w= 3, ρ_{sh} =0.0035			
0.05	0.1	0.15	0.2
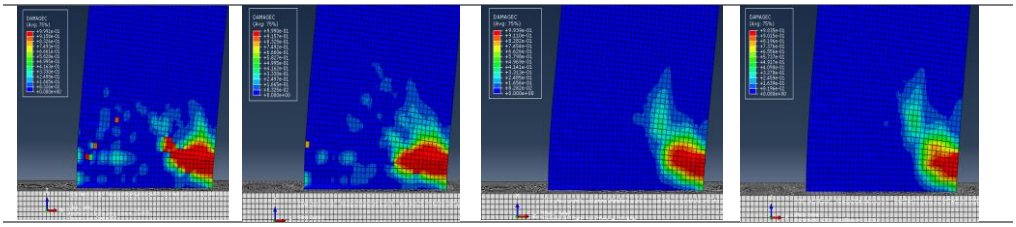			
H_w/L_w= 6, ρ_{sh} =0.0035			
0.05	0.1	0.15	0.2
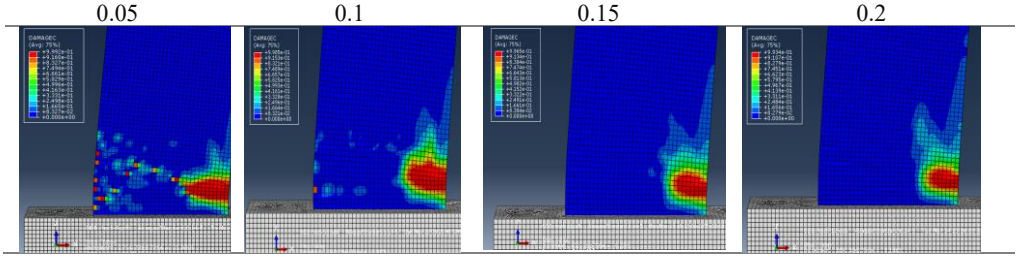			

The load-displacement curves obtained as a result of the analyzes were grouped according to N/N_o ratio. It has been observed that as the N/N_o ratio increases, the values in shear wall capacity increase. The curves include all H_w/L_w ratios considered. As the H_w/L_w ratio increased, shear wall capacities decreased. The load-displacement curves of walls with N/N_o ratio of 0.05 are shown in Figure 13-15.

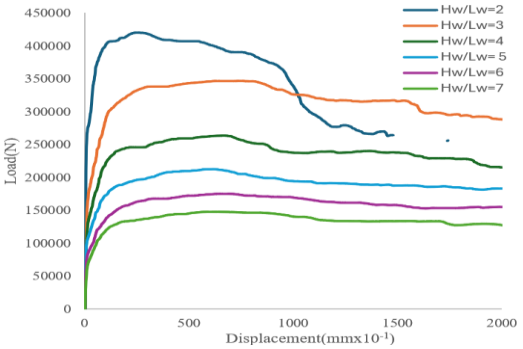

Figure 13. ρ_{sh} = 0.0015, N/N_o=0.05 load-displacement curves.

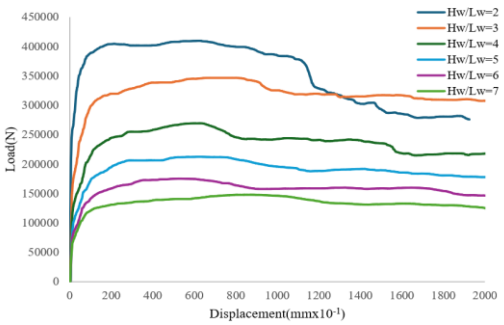

Figure 14. ρ_{sh} = 0.0025, N/N_o=0.05 load-displacement curves.

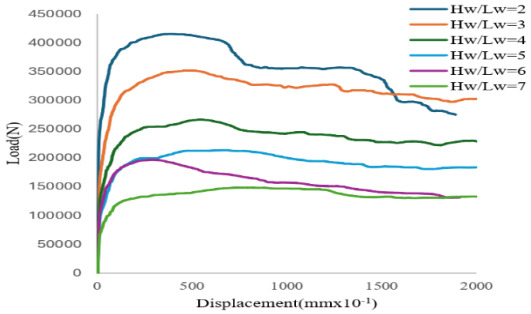

Figure 15. ρ_{sh} = 0.0035, N/N_o=0.05 load-displacement curves.

The load-displacement curves of walls with N/N_o ratio of 0.1 are shown in Figure 16-18.

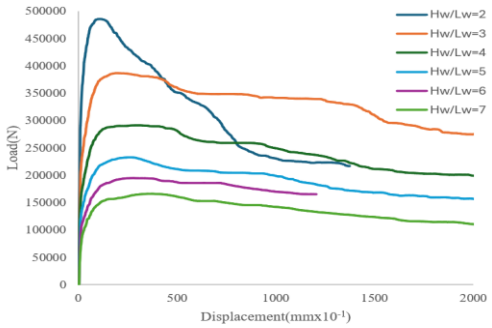

Figure 16. ρ_{sh} = 0.0015, N/N_o=0.10 load-displacement curves.

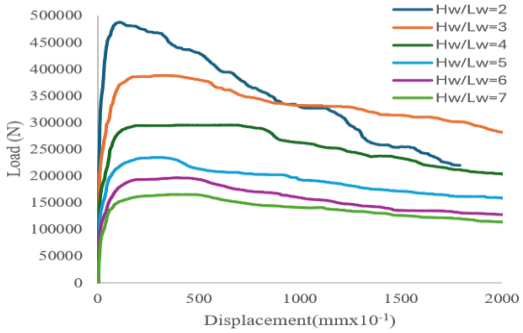

Figure 17. ρ_{sh} = 0.0025, N/N_o=0.10 load-displacement curves.

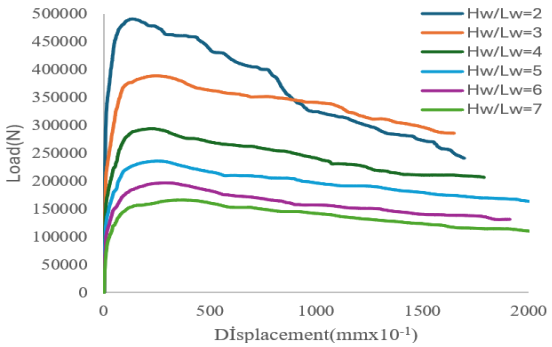

Figure 18. ρ_{sh} = 0.0035, N/N_o=0.10 load-displacement curves.

The load-displacement curves of walls with N/N_o ratio of 0.15 are shown in Figure 19-21.

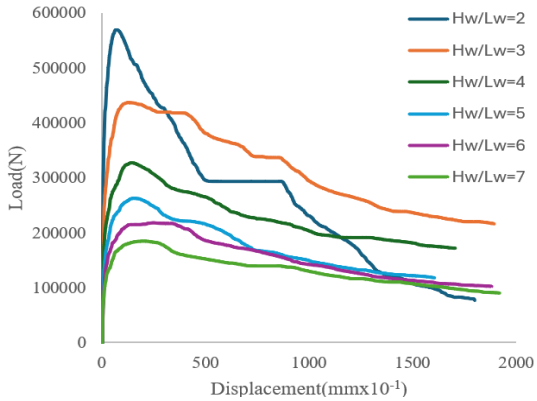

Figure 19. ρ_{sh} = 0.0015, N/N_o=0.15 load-displacement curves.

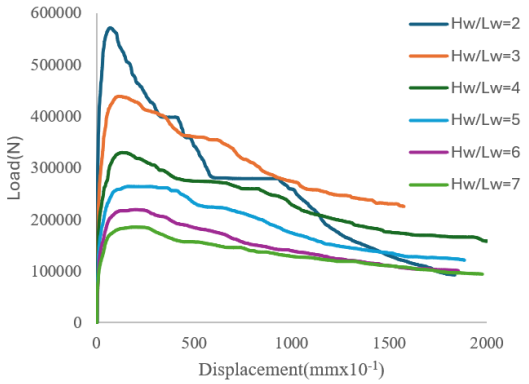

Figure 20. ρ_{sh} = 0.0025, N/N_o=0.15 load-displacement curves.

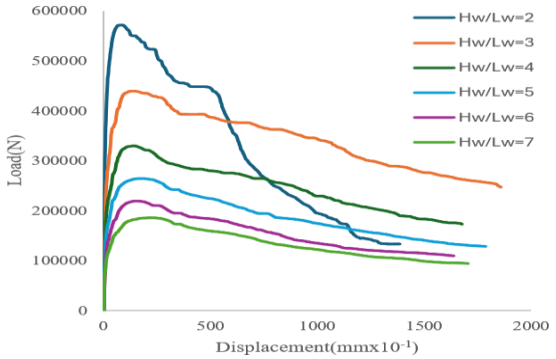

Figure 21. ρ_{sh} = 0.0035, N/N_o=0.15 load-displacement curves.

The load-displacement curves of walls with N/N_o ratio of 0.2 are shown in Figure 22-24.

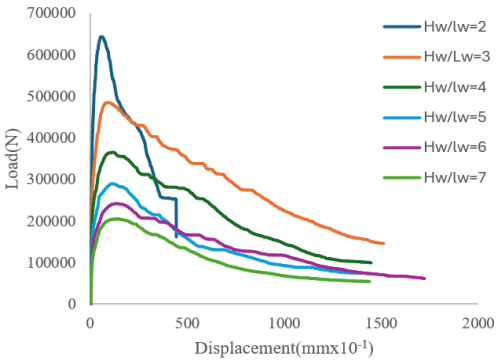

Figure 22. ρ_{sh} = 0.0015, N/N_o=0.20 load-displacement curves.

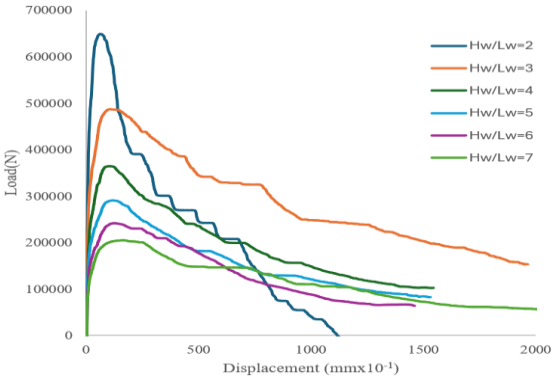

Figure 23. ρ_{sh} = 0.0025, N/N_o=0.20 load-displacement curves.

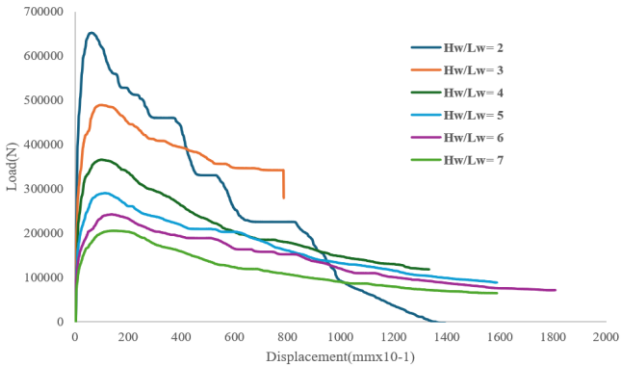

Figure 24. ρ_{sh} = 0.0035, N/N_o=0.20 load-displacement curves.

The L_p values, obtained when the maximum load decreased by 15% (0.85Fmax), were taken into account and the graphs were drawn up so that the vertical axis is L_p/L_w and the horizontal axis is H_w/L_w. The graphs grouped according to ρ_{sh} are shown in Figure 25-27. In each graph, the changes in the relations can be observed depending on N/N_o ratios. The $0.5L_w$ limiting value stated in TBEC-2018 for plastic hinge length is shown in the graphs.

The change of L_p depending on ρ_{sh} is shown in Table 8. It is seen that the horizontal web reinforcement is not a very effective parameter in the plastic hinge length. In Table 9, $(L_p/L_w)_{avg}$ values are given according to shear spans.

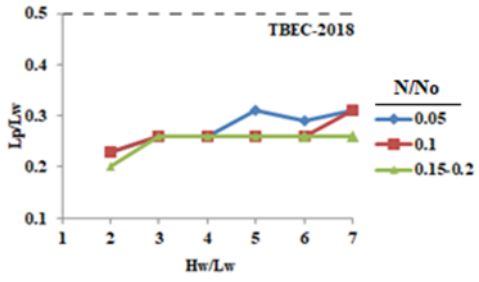

Figure 25. H_w/L_w - L_p/L_w graph for ρ_{sh} = 0.0015 (authors).

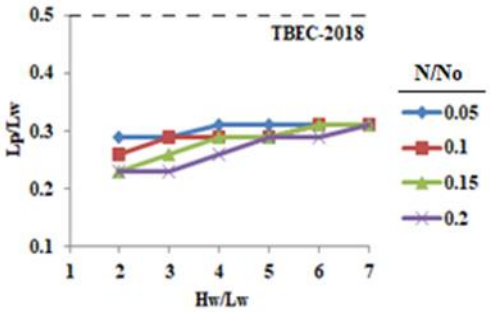

Figure 26. H_w/L_w - L_p/L_w graph for ρ_{sh} = 0.0025 (authors).

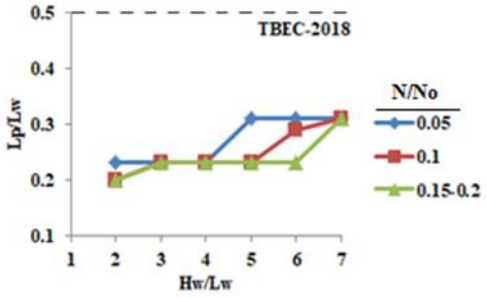

Figure 27. H_w/L_w - L_p/L_w graph for ρ_{sh} = 0.0035 (authors).

Table 8. $(L_p/L_w)_{avg}$ values according to horizontal web reinforcement ratios (authors).

Parameters	Horizontal Web Reinforcement Ratio (ρ_{sh})		
	0.0015	0.0025	0.0035
$(\frac{Lp}{Lw})_{avg}$	0.258	0.278	0.249

Table 9. $(L_p/L_w)_{ort}$ values according to shear span (authors).

Parameter	Shear Span (H_w/L_w)					
	2	3	4	5	6	7
$(\frac{Lp}{Lw})_{avg}$	0.224	0.25	0.257	0.272	0.279	0.29

When the graphs drawn up by considering the limit state are examined, it is observed that L_p values generally increase as N/N_o ratio decreases and as H_w/L_w ratio increases. It is seen that the ρ_{sh} change causes small differences and is not a very effective parameter. The value given for the plastic hinge length in TBEC-2018 is $0.5L_w$, and in the study, it was seen that plasticization occurred around $0.25\text{-}0.29L_w$. It is seen that the L_p length of the 72 shear walls analyzed within the limits in this study does not exceed the regulation limits. This shows that the code is based on a higher plastic length than the observed plasticization. On the other hand, a comparison was made according to L_{pz} values in Fig. 16-Fig-18. For each scenario taken as basis, a value greater than the plastic hinge length accepted by the code was found. For this reason, it is seen that TBEC-2018 actually defines the length of plastic hinge at a level between L_p and L_{pz}. According to the values given in Table 8 and Table 10, it is observed that L_p and L_{pz} vary in the 0.224~1.08 band.

L_{pz} obtained when the maximum load decreases by 15% were taken into consideration and the H_w/L_w vs. L_{pz}/L_w graphs were drawn up (Figures 28-30).

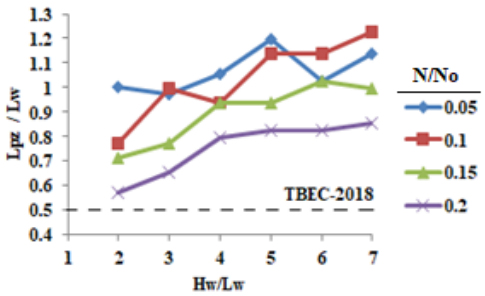

Figure 28. H_w/L_w - L_{pz}/L_w graph for ρ_{sh} = 0.0015 (authors).

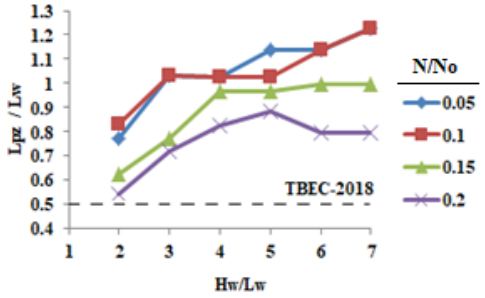

Figure 29. H_w/L_w - L_{pz}/L_w graph for ρ_{sh} = 0.0025(authors).

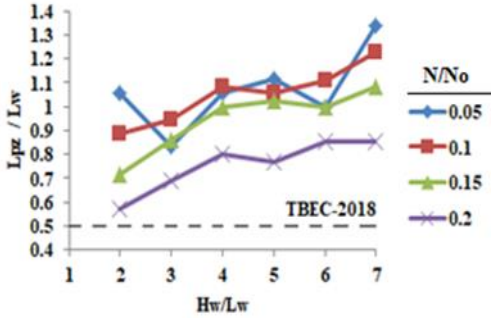

Figure 30. H_w/L_w -L_{pz}/L_w graph for $\boldsymbol{\rho}_{sh}$ = 0.0035(authors).

The effect of the ratio of N/N_o on the ratio of L_{pz}/L_w is much higher especially for the shear walls with high web reinforcement ratio (ρ_{sh}=0.0035). The decrease in the ratio of N/N_o ratio increases L_{pz} value dramatically for high H_w/L_w ratios. The change in L_{pz} with respect to ρ_{sh} is given in Table 10. Depending on the change of H_w/L_w ratio, $(L_{pz}/L_w)_{avg}$ values are shown in Table 11.

Table 10. $(L_{pz}/L_w)_{avg}$ values according to horizontal web reinforcement ratios (authors).

Parameter	Horizontal Web Reinforcement Ratio (ρ_{sh})		
	0.0015	0.0025	0.0035
$(\frac{Lpz}{Lw})_{avg}$	0.938	0.937	0.954

Table 11. $(L_{pz}/L_w)_{avg}$ values according to shearing opening (authors).

Parameter	Shear span (H_w/L_w)					
	2	3	4	5	6	7
$(\frac{Lpz}{Lw})_{avg}$	0.754	0.856	0.959	1.006	1.004	1.08

L_{pz} values decrease as N/N_o ratio increases. However, L_{pz} values increase as H_w/L_w ratio increases. The change in ρ_{sh} causes only small differences when the maximum load decreases by 15% and is not a very effective parameter. The L_p/L_{pz} and H_w/L_w ratios were determined by considering the plastic hinge lengths obtained depending on the ρ_{sh} ratio (Figure 31-33).

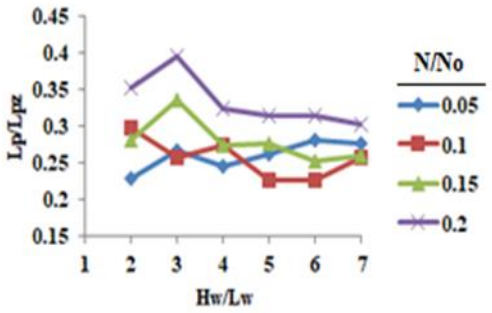

Figure 31. H_w/L_w - L_p/L_{pz} graph for $\boldsymbol{\rho}_{sh}$ = 0.0015 (authors).

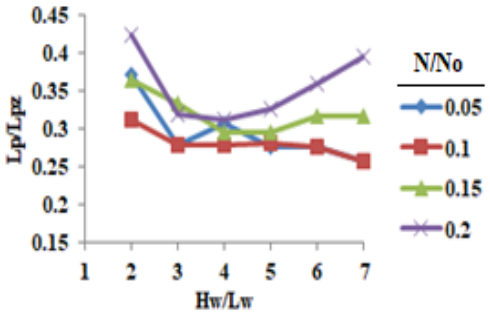

Figure 32. H_w/L_w - L_p/L_{pz} graph for $\boldsymbol{\rho}_{sh}$ = 0.0025(authors).

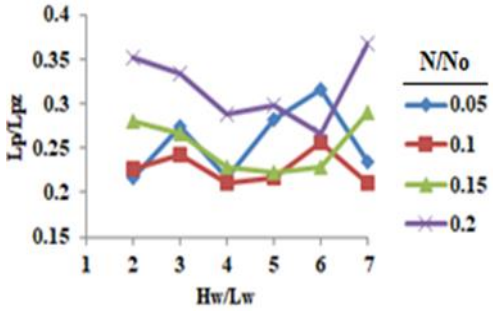

Figure 33. H_w/L_w - L_p/L_{pz} graph for ρ_{sh} = 0.0035 (authors).

It is seen that L_p and L_{pz} is related with a ratio between 0.25 and 0.4. This ratio is considered as 0.5 in the literature.

4.1. Ductility

The ductility (μ) values were determined and the H_w/L_w vs. μ graphs were created by using the displacements determined according to both the crushing occurred in the shear wall concrete and the yield observed in the steel reinforcement (Figure 34-36). Displacement ductility was determined according to the load-displacement graphs obtained for 72 walls (given in groups above, Fig 13-23). When the changes in the obtained ductility are examined, displacement ductilities ranging from 5.77 to 8.78 are observed. Of course, factors such as keeping the normal force quite limited in the study and neglecting the out-of-plane behavior of the walls caused a relative increase in ductility.

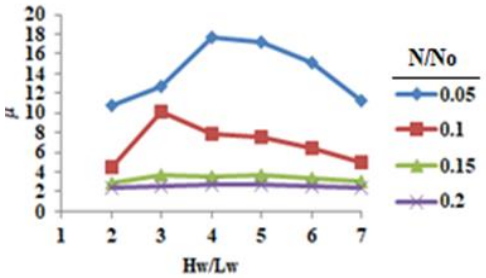

Figure 34. H_w/L_w - μ graph for ρ_{sh} = 0.0015 (authors).

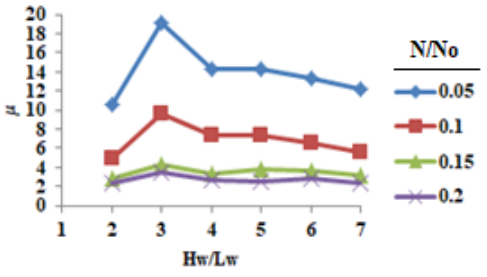

Figure 35. H_w/L_w- μ graph for ρ_{sh} = 0.0025 (authors).

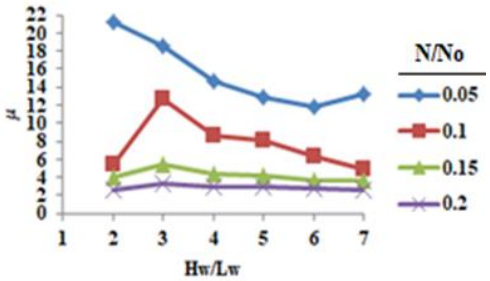

Figure 36. H_w/L_w - μ graph for ρ_{sh} = 0.0035 (authors).

The change in μ with respect to ρ_{sh} is given in Table 12. Depending on the change of H_w/L_w ratio, $(\mu)_{avg}$ values are shown in Table 13.

Table 12. $(\mu)_{avg}$ values according to horizontal web reinforcement ratios (authors).

Parameter	Horizontal Web Reinforcement Ratio (ρ_{sh})		
	0.0015	0.0025	0.0035
$(\mu)_{avg}$	6.72	6.77	7.52

Table 13. $(\mu)_{avg}$ values according to horizontal web reinforcement ratios (authors).

Parameter	Shear span (H_w/L_w)					
	2	3	4	5	6	7
$(\mu)_{avg}$	6.2	8.78	7.5	7.3	6.5	5.77

In order for the structure to exhibit ductile behavior, it must undergo plastic deformation. Since plastic hinge length and ductility are closely related, the effects of the parameters whose effects on plastic joint length were examined on ductility were also examined. It was observed that the ductility value increased as the horizontal confinement reinforcement increased. The confinement effect had a positive impact on ductility. The increase in the H_w/L_w ratio generally caused an increase in L_p and L_{pz} values. It can be said that as the H_w/l_w ratio increases, the deformations increase in the concrete and reinforcement. However, it has been observed that the ductility ratio decreases as the H_w/L_w ratio increases (except H_w/L_w=3). As the N/N_o ratio decreases, the ductility value (μ) becomes more dependent on the H_w/L_w ratio. This is more apparent especially in the shear walls having very low normal force (N/N_o = 0.05) and partially for (N/N_o = 0.1). It is also seen from the graphs that the ductility is inversely related with H_w/L_w ratio when N/N_o is less than 0.1.

4.2. Comparison of the plastic hinge lengths

The literature contains various empirical formulas for determining shear wall plastic hinge lengths and the values obtained from these equations having high number of parameters were compared with the values obtained from the finite element analyses. The comparisons were carried out the formulas proposed by EC8-2004, Biskinis and Fardis (2010) Bohl and Adebar (2011) and, Kazaz and Gülkan (2012). Both the observed plastic hinge lengths (L_p) and the analytical plastic hinge lengths (L_{pz}) were included in these comparisons. Linear curve fitting is performed and the results are shown in Figures 37-40.

The comparisons given between Figure 25 and Figure 28 were made with the results obtained from L_p formulations in the literature. The results obtained from the ABAQUS model were compared with the L_p values in the literature, within accepted limits. The point that should be noted here is that plastic hinge is stated as l_p in the literature. However, in this study, two different plastic hinge lengths were determined. For this reason, both hinge lengths obtained from this study were compared with each approach.

First of all, for each approach, it is seen that L_p matches better with the approaches in the literature compared to L_{pz}. When the R^2 values obtained from the linear regression are examined, it is seen that the best fit for the plastic hinge lengths is achieved with the study of Kazaz (2013). As shown in Figure 28, there is 78% good-fit between the values of Kazaz & Gülkan (2012) and the observed plastic hinge length values.

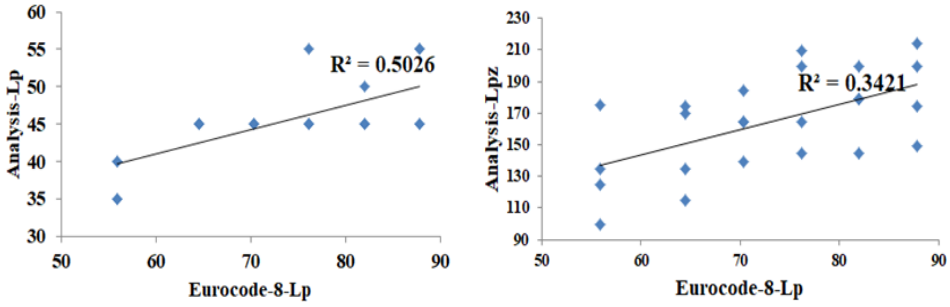

(a) (b)

Figure 37. Comparison of Eurocode-8 (2004) ; (a)with L_p (b)with L_{pz} (authors).

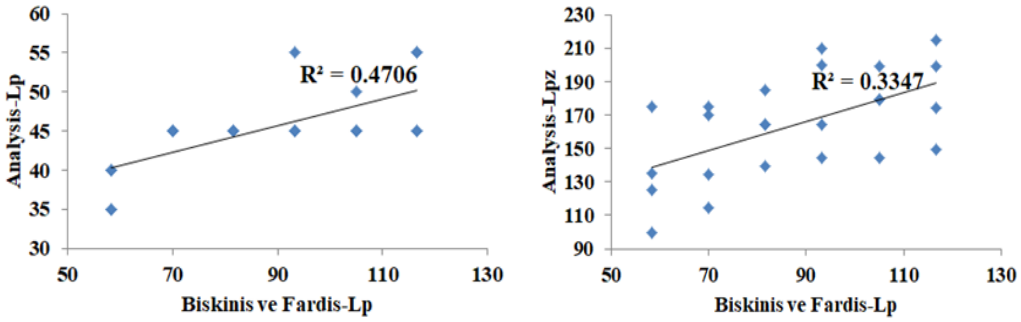

(a) (b)

Figure 38. Comparison of Biskinis & Fardis (2010) ; (a) with $L_{p,}$ (b) with L_{pz} (authors).

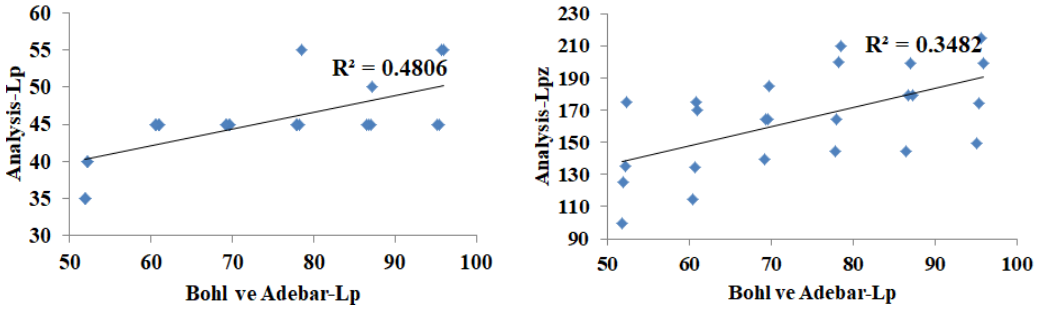

(a) (b)

Figure 39. Comparison of Bohl & Adebar (2011) ; (a) with $L_{p\ ,}$ (b)with L_{pz} (authors).

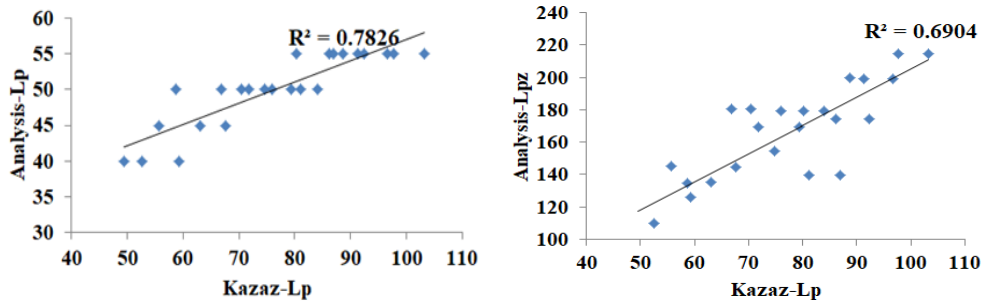

(a) (b)

Figure 40. Comparison of Kazaz & Gülkan (2012) with L_p with L_{pz} (authors).

5. Conclusions and comments

Past earthquakes have shown that the inelastic energy-consuming capacity of a shear wall is very high. For this reason, shear walls are very effective in the performance shown by the shear walled structures during an earthquake. The length of the plastic hinge that develops in the region where shear wall meet foundation depend on the dimensions and details of the shear wall. The earthquake codes make a rather simplified assumption for the length of the plastic hinge that it would depend only on the length of the shear wall in the plan and be equal to $0.5L_w$. However, in the literature, there are many empirical formulas whereby the plastic hinge length of a shear wall can be calculated. In order for the plastic hinge to emerge, the reinforcement must begin yielding.

The mechanism is realized as a result of the concrete being crushed by making excessive deformations. Therefore, regarding the plastic hinge length, there are different heights definitions: the height at which the concrete is crushed (L_p) and the hight at which the reinforcement starts yielding (L_{pz}). While L_p, which represents the region where concrete crushed, can be observed from the outside, L_{pz} cannot clearly be observed most of the time. In this study, a series of analytical studies were carried out in order to determine the relationship between L_p and L_{pz}, to identify the parameters affecting the plastic hinge length, and to compare them with the empirical approaches available in the literature. The following results were obtained from the analyses;

1) In the analyses conducted; it is seen that L_p and L_{pz} lengths increase as H_w/L_w ratio increases, and that ρ_{sh} change causes small differences in the case the maximum load decreasing by 15% and therefore, it is not a very effective parameter. It can be concluded that as the H_w/L_w ratio increases, the plastic deformations occurring in concrete and reinforcement increase. L_p were determined based on the height of observed the crush as of the foundation top level in the concrete shear wall model. It can be stated that ρ_{sh} change is not an effective parameter for L_p, because there is no confinement effect on the observed concrete damage. For L_{pz}, this situation can be explained by the fact that there are wall flange zones along the critical wall height and the reinforcement damage remains in this region.The axial force level has different effects: L_p values increase as N/N_o ratio decreases and as H_w/L_w ratio increases. It is seen that L_{pz} values decrease as N/N_o ratio increases. As the N/N_o ratio decreased, the deformation ability of concrete and reinforcement increased. When the damages occurring in concrete is examined, as N/N_o increases, the damage occurs in a narrower area. This situation can be interpreted as a decrease in ductility.

2) The value given for the plastic hinge length in TBEC-2018 is $0.5L_w$, and in the study, it was seen that plasticization occurred around $0.25\text{-}0.29L_w$. There are many different parameters that affect the height of the plastic hinge. However, considering the effects of the parameters examined, it was seen that the code remained on the safe side.

3) It is seen that L_p and L_{pz} are related with a ratio of 0.25-0.4 for the displacement limit. The literature states this ratio as 0.5. The plastic hinge length values remained between the critical shear wall heights determined by the codes. This situation can be interpreted as preventing limited ductility. The fact that the L_{pz} length is greater than the L_p length indicates that the damage occurred in the reinforcement, which is more ductile than the concrete.

4) As the N/N_o ratio decreases, the ductility value (μ) becomes more dependent on the H_w/L_w ratio. This is considerably felt especially in the shear walls having very low normal force ($N/N_o = 0.05$ and partially $N/N_o = 0.1$). It is also seen from the graphs that the ductility is inversely related to H_w/L_w ratio when N/N_o is less than 0.1. Examining the analysis results of the modeled shear walls, it is observed that the displacement ductility values decrease as the normal force value increases. The average ductility values of the shear walls, whose H_w/L_w (shear span) ratio is 2, are lower than the average ductility values of other modeled shear walls. It was observed that the ductility value was greater if the p_{sh} value was 0.0035. This may be associated with the confinement effect.

5) In the literature, there are empirical formulas to determine plastic hinge lengths, and values obtained from equations with a high number of parameters have been compared with values obtained from analyses. When the R^2 values obtained from the linear regression are examined, it is seen that the best fit for the plastic hinge lengths is achieved with the study of Kazaz (2013). The accuracy of the Kazaz approach in predicting L_p and L_{pz} values obtained by this study is 78% and 69%, respectively. It was observed that there is better agreement between the plastic hinge values obtained from the studies and the observed plastic hinge length values compared to the agreement between the plastic hinge values obtained from the studies and the analytical plastic hinge values. This finding also shows that the empirical formulas in the literature might be obtained considering the crushing of concrete.

6) Although the horizontal web reinforcement ratio does not have an effect on the plastic hinge formation and height, it is recommended by the building and seismic codes that it should be kept at a lower limit of 0.0025 to ensure that no shear damage occurs before the bending damage in the web. Similarly, since the axial force is an important factor in

the plastic hinge formation and the ductility capacity, the N/N_o ratio is limited to the upper limit of 0.35 in the codes. There is no upper limit except for the lower limit for the H_w/L_w ratio being greater than 2.0.

The results of the 72 shear walls modeled in the study can be further expanded in future studies according to the selected parameters. In this study, an evaluation was made on the parameters H_w/L_w, N/N_o, and ρ_{sh}, which are effective in shear wall behavior. Certainly, other factors may be effective in determining the behavior of shear walls. For example, wall thickness, slab type, slab-shear wall connection type are some of them. In addition, there are other which would affect the shear wall behavior such as bond-slip of the reinforcement Kazaz (2012), cyclic loading (Pokhrel & Bandelt, 2019) and the presence of slabs between the stories (He et al., 2020; Surumi et al., 2015). In future studies, machine learning-based soft computing applications can also be made using shear wall models obtained with wide range parameters. Using different machine learning methods with planned studies, predict the length of the plastic hinge will be suggested. In future studies, deriving a new analytical formula and comparing it with existing ones, in which the effects of all parameters are evaluated, could be a worthwhile way.

In reinforced concrete structures, shear walls are connected with slabs at story levels. In the studies to be developed, the behavior can be determined by adding slabs that will limit the horizontal displacement to the shear walls during the modeling phase. In the study, shear wall models were modeled as cantilever. In future studies, coupled wall models can be created and the differences between their behaviors can be examined.

The results obtained in this study were compared with the traditional results used in the literature. Ultimately, each plastic hinge model in the literature is an approach. However, in this study conducted on 72 walls, the L_p and L_{pz} lengths obtained may be more descriptive than the theoretical relations in the literature, since the section where the concrete is crushed and the reinforcement yielded can be determined from advanced non-linear FEM analyses. But the distribution of the parameters selected in this study, the range of changes, the limits in the analysis, etc. of course, this also limits their accuracy. Therefore, in future studies, comparisons can be made more sensitive with more shear wall parameters and different analysis options. The most important reason for the destruction caused by the earthquakes that occurred in Turkey on February 6, 2023, more than 50,000 people died and causing economic losses of nearly ten billion dollars, is the absence of well-designed (the seismic code design criteria proper) shear walls in reinforced concrete buildings. Therefore, studies conducted in the coming years regarding reinforced concrete shear walls will provide valuable insights for reinforced concrete buildings with better earthquake behavior.

Author contributions: Each author contributed to the design and implementation of the research, to the analysis of the results and to the writing of the manuscript.

Funding: Authors especially would like to thank Konya Technical University BAP (Project Number: 191004005)

Conflicts of interest: The authors declare that they have no conflict of interest.

References

ACI Committee 318. (2019). Building Code Requirements for Structural Concrete and Commentary (ACI 318-A9). In American Concrete Institute. American Concrete Institute. https://doi.org/10.14359/51716937

Aksoylu, C., Mobark, A., Arslan, M. H. and Erkan, I. H. (2020). A comparative study on ASCE 7-16, TBEC-2018 and TEC-2007 for reinforced concrete buildings. Revista de la Construcción. Journal of Construction. 19(2), 282-305. http://dx.doi.org/10.7764/rdlc.19.2.282 Alkazan, E. (2020). Effect of shear wall ratio on the force distribution in structures. (Master Thesis), Erzurum Technical University.

Altheeb, A., Albidah, A., LAM, N., & Wilson, J. (2015). Analytical modelling of strain penetration deformation in reinforced concrete members. Proceedings of the Tenth Pacific Conference on Eartquake Engineering Builging an Eartquake- Resilient, November.

Arslan, M. H. (2012). Estimation of curvature and displacement ductility in reinforced concrete buildings, KSCE Journal of Civil Engineering, 16(5):759-770.

Aydın, S. (2018). Evaluation of plastic hinge length estimations and strain limits of reinforced concrete shear walls. (Master's Thesis),Istanbul Technical University, Institute of Science Engineering and Technology.

Barbagallo, F., Bosco, M., Floridia, A., Marino, E.M., Panarelli, D.,Rossi, P.P., & Spinella, N. Calibration of the length of the plastic hinge for numerical models of reinforced concrete members. Buildings 2022, 12, 1603. https://doi.org/10.3390/ buildings12101603

Biskinis, D., & Fardis, M. N. (2010). Flexure-controlled ultimate deformations of members with continuous or lap-spliced bars. Structural Concrete, 11(2), 93–108. https://doi.org/10.1680/stco.2010.11.2.93

Bohl, A., & Adebar, P. (2011). Plastic hinge lengths in high-rise concrete shear walls. ACI Structural Journal, 108(2), 148–157.

Burak, B, & Comlekoglu, H. G. (2013). Effect of shear wall area to floor area ratio on the seismic behavior of reinforced concrete buildings. J. Struct. Eng, 139 (2013) 1928–1937.

Cai, W. Z., Wang, B., Shi, Q. X., & Wu, M. Z. (2024). Plastic hinge length for flanged reinforced concrete shear walls with asymmetric sections. Journal of Earthquake Engineering, 28:10, 2883-2908. https://doi.org/10.1080/13632469.2024.2314699

Cheng, Y., He, H., Sun, H., & Cheng, S. Experimental study and mechanism analysis of out-of-plane seismic performance of reinforced concrete shear walls. Journal of Building Engineering, 80 (2023) 108058. 80 (2023) 108058

Clauß F., Ahrens, M. A.,& Mark P. (2021). A comparative evaluation of strain measurement techniques in reinforced concrete structures–A discussion of assembly, application, and accuracy. Structural Concrete, 22: 2992–3007. https://doi.org/10.1002/suco.202000706

Dazio, A., Beyer, K., & Bachmann, H. (2009). Quasi-static cyclic tests and plastic hinge analysis of RC structural walls. Engineering Structures, 31(7), 1556–1571. https://doi.org/10.1016/j.engstruct.2009.02.018

Değer, Z., & Başdoğan, Ç. (2020). Betonarme perdelerin yığılı plastik davranış ile doğrusal olmayan modellenmesi ve hasar sınırları. Gazi Üniversitesi Mühendislik-Mimarlık Fakültesi Dergisi, 36(2), 641–653. https://doi.org/10.17341/gazimmfd.719923

Dere, Y. (2017). Assessing a retrofitting method for existing RC buildings with low seismic capacity in Turkey. Journal of Performance of Constructed Facilities, 31(2). https://doi.org/10.1061/(ASCE)CF.1943-5509.0000969

El-Hashimy, T., Ezzeldin, M. El-Dakhakhni, W., & Tait, M.(2020). Behavior of seismically detailed reinforced concrete block shear walls with boundary elements under out-of-plane loading. J. Struct. Eng., 2020, 146(3): 04020005.

En 1998-1. (2004). Eurocode8: Design of structures for earthquake resistance - Part 1: General rules, seismic actions and rules for buildings. European Committee for Standardization.

Encina, E., Lu, Y., & Henry, R. S. (2016). Axial elongation in ductile reinforced concrete walls. Bulletin of the New Zealand Society for Earthquake Engineering, 49(4), 305–318. https://doi.org/10.5459/bnzsee.49.4.305-318

Eslami, A., & Ronagh, H. R. (2014). Effect of elaborate plastic hinge definition on the pushover analysis of reinforced concrete buildings. The Structural Design of Tall and Special Buildings, 23(4), 254–271. https://doi.org/10.1002/tal.1035

Foroughi, S., & Yüksel, S. B. (2019). Investigation of displacement behavior of reinforced concrete shear walls with different plastic hinge relationships. International Journal of Eastern Anatolia Science Engineering and Design, 1(2), 196–211. https://dergipark.org.tr/tr/pub/ijeased

Foroughi, S., & Yüksel, S. B. (2020). Investigation of nonlinear behavior of high ductility reinforced concrete shear walls. International Advanced Researches and Engineering Journal, 04(02), 116–128. https://doi.org/10.35860/iarej.693724

Gallegos, M. F., Araya-Letelier, G., Lopez-Garcia, D., & Parra, P.F. (2023). Seismic collapse performance of high-rise RC dual system buildings in subduction zones. Case Studies in Construction Materials, 18 (2023) e02042. https://doi.org/10.1016/j.cscm.2023.e02042

Grossi, P., Williams, C., Cabrera, C., Tabucchi, T., Sarabandi, P., Rodríguez, A., Aslani, H., & Rahnama, M. (2011). The 2010 Maule, Chile Earthquake: Lessons and Future Challenges. In Risk Management Solutions Inc.

Hashim, D., Al-Attar, A., & Kzar, N. (2020). Investigation of plastic hinge length of reinforced concrete wall. Proceedings of the Proceedings of the 1st International Multi-Disciplinary Conference Theme: Sustainable Development and Smart Planning, IMDC-SDSP 2020, Cyperspace, 28-30 June 2020. https://doi.org/10.4108/eai.28-6-2020.2298214

He, J., Chen, J., Ren, X., & Li, J. (2020). A shake table test study of reinforced concrete shear wall model structures exhibiting strong non-linear behaviors. Engineering Structures, 212, 110481. https://doi.org/10.1016/j.engstruct.2020.110481

Henry, R. S. (2013). Assessment of minimum vertical reinforcement limits for RC walls. Bulletin of the New Zealand Society for Earthquake Engineering, 46(2), 88–96. https://doi.org/10.5459/bnzsee.46.2.88-96

Hoffmann, K. 2012.An introduction to stress analysis using strain gauges – the definitive work on strain gauge measurement. 2012

Hoult, R., Goldsworthy, H., & Lumantarna, E. (2018). Plastic hinge length for lightly reinforced rectangular concrete walls. Journal of Earthquake Engineering, 22(8), 1447–1478. https://doi.org/10.1080/13632469.2017.1286619

Istanbul Technical University. 2023. 2023 Final Earthquake Report from ITU. Accessed May 17, 2023. https://haberler. itu.edu.tr/docs/default-source/default-document-library/2023_itu_subat_2023_deprem_son_raporu.pdf?sfvrsn= 1583fe76_2

Inel, M., Ozmen, H.B.(2006). Effect of plastic hinge properties in nonlinear analysis of reinforced concrete buildings, Engineering Structures, 28 (2006) 1494–1502.

Jun, D. H. (2014). Nonlinear analysis of reinforced concrete shear wall using fiber elements. In G. M. A. Cunha, E. Caetano, P. Ribeiro (Ed.), Proceedings of the 9th International Conference on Structural Dynamic , EURODYN 2014, Vols. 2014-Janua, Issue July, pp. 523–528.

Kam, W. Y., Pampanin, S., & Elwood, K. (2011). Seismic performance of reinforced concrete buildings in the 22 february christchurch (Lyttelton) earthquake. Bulletin of the New Zealand Society for Earthquake Engineering, 44(4), 239–278. https://doi.org/10.5459/bnzsee.44.4.239-278

Kazaz, I. (2012). Betonarme perde duvarların sonlu eleman analizinde aderans kaymasının uygulanması(Application of Bond-Slip in the Finite Element Analyses of Reinforced Concrete Shear Walls). Pamukkale Üniversitesi Mühendislik Bilimleri Dergisi, 18(3), 155–163.

Kazaz, I., & Gülkan, P. (2012). Süneklik düzeyi yüksek betonarme perdelerdeki hasar sınırları. Teknik Dergi/Technical Journal of Turkish Chamber of Civil Engineers, 23(114), 6113–6140. https://dergipark.org.tr/en/pub/tekderg/issue/12745/155147.

Kazaz, I. (2013). Analytical study on plastic hinge length of structural walls. Journal of Structural Engineering, 139(11), 1938–1950. https://doi.org/10.1061/(ASCE)ST.1943-541X.0000770

Kazaz, I. (2016). Seismic deformation demands on rectangular structural walls in frame-wall systems. Earthquakes and Structures, 10 (2016) 329–350. https://doi.org/10.12989/EAS.2016.10.2.329.

Kumbasaroğlu, T. (2010). Az ve orta katlı mevcut binaların güçlendirilmesine ilişkin bir öneri.

Ling, J. H., Lim, Y.T. & Jusli, E. 2023. Methods to determine ductility of structural members: a review. Journal of the Civil Engineering Forum, May 2023, 9(2):181-194.

Lu, Y., Gultom, R. J., Ma, Q. Q., & Henry, R. S. (2018). Experimental validation of minimum vertical reinforcement requirements for ductile concrete walls. ACI Structural Journal, 115(4), 1115–1130. https://doi.org/10.14359/51702048

Lu, Y., Henry, R. S., Gultom, R., & Ma, Q. T. (2017). Cyclic testing of reinforced concrete walls with distributed minimum vertical reinforcement. Journal of Structural Engineering, 143(5). https://doi.org/10.1061/(ASCE)ST.1943-541X.0001723

Marius, M. (2013). Seismic behaviour of reinforced concrete shear walls with regular and staggered openings after the strong earthquakes between 2009 and 2011. Engineering Failure Analysis, 34 (2013) 537–565. http://dx.doi.org/10.1016/j.engfailanal.2013.05.014

Mamdouh, H., Zenhom, N., Hasabo, M., Deifalla, A.F., & Salman, A. (2022). Performance of strengthened reinforced concrete shear walls with opening. Sustainability, 14, 14366. https://doi.org/10.3390/su142114366

Marzok, A., Lavan, O., & Dancygier, A. N. (2020). Predictions of moment and deflection capacities of RC shear walls by different analytical models. Structures, 26(April), 105–127. https://doi.org/10.1016/j.istruc.2020.03.059

Massone, L. M., & Alfaro, J. I. (2016). Displacement and curvature estimation for the design of reinforced concrete slender walls. The Structural Design of Tall and Special Buildings, 25(16), 823–841. https://doi.org/10.1002/tal.1285

Ozdemir, A., Kopraman, Y., & Anıl, Ö. (2021). Hysteretic behavior of retrofitted RC shear wall with different damage levels by using steel strips. Journal of Building Engineering, 44(July), 103394. https://doi.org/10.1016/j.jobe.2021.103394

Oztürk, M., Arslan, M. H. & Korkmaz, H. H. (2023). Effect on RC buildings of 6 February 2023 Turkey earthquake doublets and new doctrines for seismic design. Engineering Failure Analysis, Volume 153, 107521. https://doi.org/10.1016/j.engfailanal.2023.107521

Oztürk, M., Arslan M. H., Dogan, G., Ecemis, A.S. & Arslan, H. D. (2023). School buildings performance in 7.7 Mw and 7.6 Mw catastrophic earthquakes in southeast of Turkey. Journal of Building Engineering, Volume 79.

Pokhrel, M., & Bandelt, M.J. (2019) Predicting UHPC structural response at ultimate limit state through numerical simulation technique. International Interactive Symposium on Ultra-High Performance Concrete 2(1).https://doi.org/10.21838/uhpc.9691

Pokhrel, M., & Bandelt, M. J. (2019). Plastic hinge behavior and rotation capacity in reinforced ductile concrete flexural members. Engineering Structures, 200, 109699. https://doi.org/10.1016/j.engstruct.2019.109699

Priestly, M. J., Calvi, G., & Kowaisky, M. J. (2007). Displacement-based seismic design of structures. IUSS Press.

Robazza, B. R., Brzev, S., Yang, T. Y., Elwood, K. J., Anderson, D. L., & McEwen, B. (2018). Out-of-plane behavior of slender reinforced masonry shear walls under in-plane loading: experimental investigation. J. Struct. Eng., 2018, 144(3): 04018008.

Sorosh, S., & Sari, A. (2022). Numerical investigation of the lateral load behavior of core and coupled rocking walls. Revista de La Construcción. Journal of Construction, 21(1), 36–52. https://doi.org/10.7764/RDLC.21.1.36

Soydaş, O. (2009). Evaluation of shear wall indexes for reinforced concrete buildings. (Master Thesis), Middle East Technical University. https://hdl.handle.net/11511/18466.

Sritharan, S., Beyer, K., Henry, R. S., Chai, Y. H., Kowalsky, M., & Bull, D. (2014). Understanding poor seismic performance of concrete walls and design implications. Earthquake Spectra, 30(1), 307–334. https://doi.org/10.1193/021713EQS036M

Surumi, R. S., Jaya, K. P., & Greeshma, S. (2015). Modelling and assessment of shear wall–flat slab joint region in tall structures. Arabian Journal for Science and Engineering, 40(8), 2201–2217. https://doi.org/10.1007/s13369-015-1720-z

Takahashi, S., Yoshida, K., Ichinose, T., Sanada, Y., Matsumoto, K., Fukuyama, H., & Suwada, H. (2013). Flexural drift capacity of reinforced concrete wall with limited confinement. ACI Structural Journal, 110(1), 95–104. https://doi.org/10.14359/51684333

TBEC. (2018). Turkish Building Earthquake Code Specifications for Design of Buildings under Seismic Effects. 1–416. https://www.resmigazete.gov.tr/eskiler/2018/03/20180318M1-2-1.pdf

Thomsen, J. H., & Wallace, J. W. (2004). Displacement-based design of slender reinforced concrete structural walls—experimental verification. Journal of Structural Engineering, 130(4), 618–630. https://doi.org/10.1061/(ASCE)0733-9445(2004)130:4(618)

Wang, W., Luo, Q., Sun, Z., Wang, B. & Xu, S. Relation analysis between out-of-plane and in-plane failure of corrugated steel plate shear wall. Structures 29 (2021) 1522–1536. https://doi.org/10.1016/j.istruc.2020.12.030

Wei, L. Tan, W., & Wang, W. T. (2017). Out of plane seismicdesign of shear wall in Y direction for shear wall structure with few walls in X direction, Build. Srruct.47(1) 28-32.

Westenenk, B., de la Llera J.C., Jünemann, R., Hube, M., & Besa, J. J. (2012). Seismic response of reinforced concrete buildings in Concepción during the Maule earthquake. 15th World Conference on Eartquake Engineering 2012 (15WCEE), 28(S1), S257-S280.

Zhao,X., Wu, Y., Leung, A.Y., & Lam, H. F.(2011). Plastic hinge length in reinforced concrete flexural members. Procedia Engineering 14 (2011) 1266–1274.

Zhang, X., Zhou, G., Li, S., Zhang, F., & Zhang,S. (2022). Experimental and numerical study on seismic behavior of prestressed concrete composite shear wall. Engineering Structures. 266 (2022) 114546. https://doi.org/10.1016/j.engstruct.2022.114546

Zhi, Q., Zhou, B., Zhu, Z., & Guo, Z. (2019). Evaluation of load–deformation behavior of reinforced concrete shear walls with continuous or lap-spliced bars in plastic hinge zone. Advances in Structural Engineering, 22(3), 722–736. https://doi.org/10.1177/1369433218798717.

Copyright (c) 2024. Tülen, H., Dere Y., Arslan, M.H. This work is licensed under a Creative Commons Attribution-Noncommercial-No Derivatives 4.0 International License.